**Rare Metal Materials and Engineering**
Volume 51, Issue 12, December 2022
Available online at www.rmme.ac.cn

Science Press

**Cite this article as**: Li Yanxing, Wang Lin, An Rui, et al. Deformation Behavior of Ti-6Al-3Nb-2Zr-1Mo Titanium Alloy at Low Temperatures and High Strain Rates[J]. Rare Metal Materials and Engineering, 2022, 51(12): 4369-4375.

ARTICLE

# Deformation Behavior of Ti-6Al-3Nb-2Zr-1Mo Titanium Alloy at Low Temperatures and High Strain Rates

**Li Yanxing[1], Wang Lin[1,2,3], An Rui[1], Zhao Pingluo[1], Yan Zhiwei[1], Cheng Huanwu[1,2], Cheng Xingwang[1,2]**

*[1] School of Materials Science and Engineering, Beijing Institute of Technology, Beijing 100081, China; [2] National Key Laboratory of Science and Technology on Materials Under Shock and Impact, Beijing Institute of Technology, Beijing 100081, China; [3] State Key Laboratory of Explosion Science and Technology, Beijing Institute of Technology, Beijing 100081, China*

**Abstract:** Dynamic compression tests of Ti6321 titanium alloy were carried out in the temperature range from 193 K to 298 K and strain rate range from 2000 $s^{-1}$ to 3000 $s^{-1}$ to study the effects of temperature and strain rate on the mechanical properties and deformation behavior of the alloy. The microstructure evolution was observed and analyzed by optical microscope (OM), transmission electron microscope (TEM) and electron backscatter diffraction (EBSD). The results show that with decreasing temperature and increasing strain rate, dynamic yield strength and average flow stress of Ti6321 titanium alloy increase, while the fracture strain decreases obviously. Johnson-Cook constitutive equation is used to predict the mechanical behavior at low temperatures and high strain rates, and the fitting results are in good agreement with the experimental ones. Microstructural study shows that the content of the $\{11\bar{2}\bar{1}\}$ and $\{10\bar{1}2\}$ extension twins increases significantly as the deformation temperature decreases. The deformation mechanism gradually changes from the auxiliary role of twins to the dominance of twins.

**Key words:** Ti6321 titanium; low temperatures; high strain rates; microstructure evolution; deformation mechanism

Titanium alloys are widely used in deep submersibles, ships, and submarines because of their high specific strength and good corrosion resistance[1-3]. In addition, titanium alloys offer a range of advantages such as low thermal conductivity, low coefficient of expansion and low-temperature resistance, which make them ideal as cryogenic materials in industrial applications such as ships[4-6]. In these fields, titanium alloys are commonly used in the manufacture of pressure-resistant housings, propellers, and sonar deflector shields. These components are often subjected to a load combination of low temperatures and high strain rate during service[7,8]. Therefore, it is of great engineering importance to understand the mechanical behavior and microstructure evolution of titanium alloys under high loading rates at low temperatures.

The main low-temperature titanium alloys used at present are Ti-5Al-2.5Sn (TA7), Ti-6Al-4V ELI, and CT20 (Ti-Al-Zr-Mo series)[9,10], among which the near-$\alpha$ titanium alloy CT20 has been used in engine liquid hydrogen piping systems due to its excellent welding and cold forming properties[11]. It has been shown that $\alpha$ titanium alloys have better low-temperature properties than $\alpha+\beta$ titanium alloys, mainly due to twinning-induced plasticity at low temperatures[12]. Near-$\alpha$ titanium alloys combine the advantages of these two alloys and are widely used in cryogenic applications. So it is important to study the deformation behavior characteristics of near-$\alpha$ titanium alloys at low temperatures for their wider application.

Some research has been carried out on the mechanical behavior of titanium alloys at high strain rates or low temperatures. Zhang et al[13,14] conducted low-temperature tensile tests on Ti-6.6Al-3.3Mo-1.8Zr-0.29Si titanium alloy and Ti-5Al-2.5Sn titanium alloy in the strain rate range of 0.001~1150 $s^{-1}$ and temperature interval of 153~298 K using the split Hopkinson tension bar (SHTB). The results showed that the low-temperature behavior of titanium alloys depends on the strain rate and temperature. The initial yield stress and flow stress increase with increasing the strain rate and

Received date: March 08, 2022
Foundation item: State Key Laboratory of Explosive Science and Technology Fund (YBKT17-06)
Corresponding author: Wang Lin, Ph. D., Associate Professor, School of Materials Science and Engineering, Beijing Institute of Technology, Beijing 100081, P. R. China, Tel: 0086-10-68912709, E-mail: linwang@bit.edu.cn

decreasing temperature. The isothermal strain-hardening behavior does not change much at different strain rates and temperatures. The adiabatic temperature rise is the main reason for the decrease in the strain-hardening rate during high-speed deformation. Gao et al[15] explored the effects of high strain rate and low temperature on the mechanical properties and deformation mechanism of industrial pure titanium TA2. The results showed that under the combined effect of high strain rate and low temperature, TA2 is brittle, with increased strength and greatly reduced plasticity. Ning et al[16] found that Ti6321 titanium alloy has a significant strain rate strengthening effect at high strain rates and analyzed its adiabatic shear behavior. Lu[17] and Zang[18] et al researched the deformation mechanism of near-$\alpha$ titanium alloys at low temperatures. Experimental results indicated that twins are more easily activated at cryogenic temperatures. The twinning deformation improves the plastic deformation capacity of titanium alloy by coordinating the crystallo-graphic orientation, promoting the boundary rotating and the dislocation slipping abilities.

The existing research show that the strength of near-$\alpha$ titanium alloys increases with decreasing temperature and increasing strain rate. However, the mechanical behavior and microstructural evolution of near-$\alpha$ titanium alloys under high strain rate and low temperature conditions is seldom reported. Therefore, considering that the marine titanium alloy sheets need to face impact loads and environmental conditions in engineering applications from 193 K to room temperature, it is of theoretical and engineering significance to experimentally investigate the compressive properties of near-$\alpha$ titanium alloys under high strain rate and low temperature conditions. The near-$\alpha$ titanium alloy Ti6321 is a medium strength and high toughness titanium alloy with a nominal composition of Ti-6Al-3Nb-2Zr-1Mo, which has good corrosion resistance, fatigue resistance, and low-temperature resistance and is widely used in marine applications[19,20]. In this study, the deformation and damage behavior of Ti6321 titanium alloy with a bimodal structure at low temperatures were investigated using a modified split Hopkinson pressure bar (SHPB) as a loading device.

## 1 Experiment

Ti6321 titanium alloy sheet in the hot-rolled state was subjected to solid solution treatment at 960 °C for 1 h, followed by air cooling. The obtained microstructure is shown in Fig.1. The microstructure consists of a lamellar secondary $\alpha$ phase diffusely distributed in the $\beta$ matrix and an equiaxed primary $\alpha$ phase.

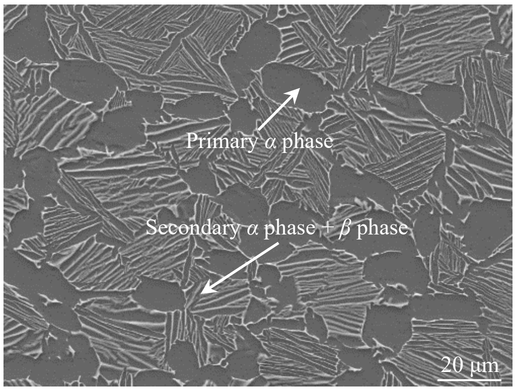


Fig.1 Microstructure of Ti6321 titanium alloy after heat treatment

The sample for dynamic compression was a cylinder of $\Phi$5 mm×5 mm. The loading device was a split Hopkinson pressure bar with the addition of a cryogenic device, as shown in Fig.2. During the test, the samples were fixed with plastic foam and placed inside a cylindrical sleeve, and the entire sleeve was placed in the SHPB low-temperature liquid nitrogen test system. The system controlled the temperature change by changing the amount of liquid nitrogen input to keep the temperature constant around the set value. The temperatures were set to 253 and 193 K. After the temperature was stabilized, liquid nitrogen was continuously introduced and maintained for 30 min. By adjusting the gas valve, the samples were dynamically compressed at different air pressures to achieve strain rates of about 2000, 2500, and 3000 $s^{-1}$ to obtain stress-strain curves for different strain rates of compression. The samples were recovered for microstructure observation. In addition, the dynamic compression test was conducted at room temperature, and the low temperature experiment was used as a comparison to study the deformation and damage behavior of Ti6321 titanium alloy in the temperature range of 193~298 K.

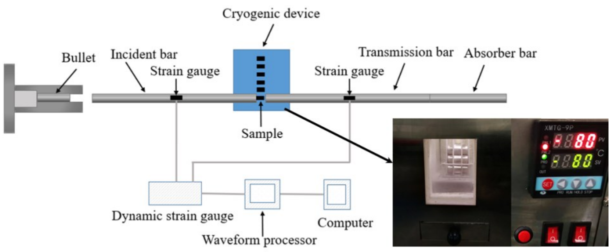


Fig.2 Experimental setup and schematic diagram

## 2 Results and Discussion

### 2.1 Mechanical properties

Fig. 3a shows the true stress-strain curves of Ti6321 alloy under different conditions. It can be seen that the true stress-strain curve consists of elastic deformation period, plastic deformation period and fracture period. With the gradual increase in the strain, the flow stress rises rapidly to the yield point and then enters into the uniform plastic deformation period. The flow stress fluctuates within a small range, which is mainly due to the interaction between work-hardening effect and thermal softening effect. Then, the effect of thermal softening effect exceeds the strain hardening effect, so the alloy undergoes thermal viscoplastic instability, an adiabatic shear zone is generated, and the load-bearing capacity of the material decreases, which eventually causes shear damage failure. In addition, Fig. 3a shows that as the temperature

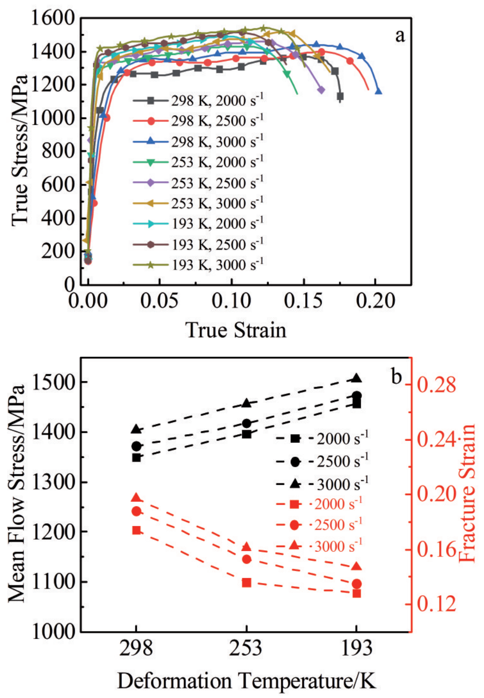


Fig.3 Variation of mechanical behavior of Ti6321 alloy at different temperatures and strain rates: (a) true stress-strain curves and (b) average flow stress and fracture strain

decreases, the elastic deformation decreases and the slope of the elastic phase increases. This indicates that the lower the temperature, the more difficult to produce elastic deformation, i.e., the greater the stiffness of the alloy.

The yield stress and flow stress of Ti6321 alloy are above 1200 MPa under different strain rate loadings. As the strain rate increases, the yield point rises, and both the flow stress and plastic strain increase, showing a certain strain-rate hardening effect, which indicates that Ti6321 titanium alloy is a strain-rate sensitive material. As shown in Fig. 3b, the average flow stress increases approximately linearly with decreasing temperature, while the fracture strain decreases.

The constitutive model is vital for the description of the mechanical behavior under different loading conditions. Several constitutive models have been developed to characterize the mechanical behavior during deformation. Among them, the J-C constitutive model has a simple form, a few parameters, ease of use, and a better description of the strain hardening, strain rate effects, and thermal softening effects of materials[21-24]. It is widely used in engineering. The J-C constitutive model is expressed as:

$$\sigma = (A + B\varepsilon^n)(1 + C\ln\dot{\varepsilon}^*)[1 - (T^*)^m] \tag{1}$$

where $\sigma$ is equivalent stress, $\varepsilon$ is equivalent plastic strain, $A$ is yield stress of the material under reference deformation conditions (MPa), $B$ is strain hardening constant (MPa), $n$ is strain hardening coefficient, $C$ is strain rate strengthening coefficient and $m$ is thermal softening coefficient. $\dot{\varepsilon}^*$ is calculated by the division of equivalent strain rate to reference strain rate and $T^*$ is dimensionless temperature, which is defined as:

$$T^* = \frac{T - T_R}{T_M - T_R} \tag{2}$$

where $T_R$ is the reference temperature and $T_M$ is the melting temperature. This research focuses on the mechanical behavior of titanium alloys under low temperature and high strain rate loading, so a reference temperature of 193 K and a reference strain rate of 2000 $s^{-1}$ were selected.

This research is based on the clustering global optimization algorithm for fitting the parameters of the present constitutive equations. The global optimization algorithm constructs a computational method to find the global optimal solution of a multivariate nonlinear function in a constrained region. The problem of determining the parameters of the J-C constitutive equation is actually the optimal solution of nonlinear functions. So the global optimization algorithm is well suited for the determination of the parameters, and it has the advantages of saving time and effort and high accuracy of fitting.

The approximate process of fitting is as follows. Firstly, the corresponding stress-strain curves are obtained experimentally, and the curves are processed to remove their elastic and failure segments. Then, the processed data are input into the corresponding software for solving. $A$, $B$, $n$, $C$, and $m$ in the J-C constitutive equation are used as optimization variables in the clustering global optimization algorithm. For the reference temperature and strain rate of this study, parameter $A$ is 1358 MPa, so four parameters such as $B$, $n$, $C$, and $m$ actually need to be optimized. The software automatically fits the experimental and theoretically calculated stress-strain curves by the global optimization algorithm. The optimal solution is obtained when the optimization results reach the set convergence threshold, i. e., when the error between the experiment and the fit is minimized.

The parameters of the fitted J-C constitutive are shown in Table 1.

J-C constitutive equation for Ti6321 alloy at low temperature and high strain rate was obtained by substituting the parameters into Eq. (1). The results of fitting the constitutive parameters at different temperatures and strain rates are compared with the experiments, as shown in Fig. 4. The overall error of the fitted results is calculated to be within 5%, which is in good agreement with the experimental data. This constitutive model can be used to simulate the mechanical properties of Ti6321 alloy at low temperatures and high strain rates.

### 2.2 Microstructure evolution

Fig.5a shows the TEM micrograph of the original structure, from which it can be seen that the lamellar structure in the bimodal structure consists of $\alpha$ phase (width of 0.2~0.5 μm) and $\beta$ phase (width of about 0.1 μm). During the deformation process, the fine $\beta$ phase layer first shows a certain

**Table 1 Parameters of the J-C constitutive equation**

| $A$/MPa | $B$/MPa | $n$ | $C$ | $m$ |
|---|---|---|---|---|
| 1358 | 491 | 0.585 | 0.0754 | 0.917 |

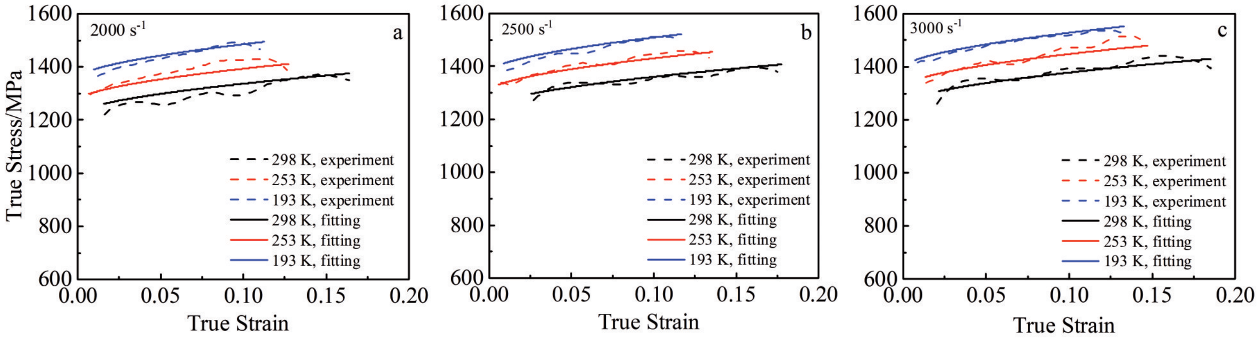


Fig.4 Fitting results of the J-C constitutive model parameters of Ti6321 alloy at different strain rates: (a) 2000 $s^{-1}$, (b) 2500 $s^{-1}$, and (c) 3000 $s^{-1}$

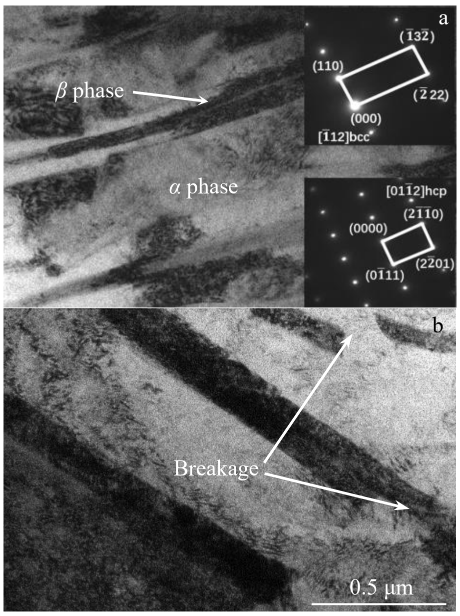


Fig.5 TEM images of Ti6321 alloy before (a) and after (b) deformation

deformation under the action of external force and then partially undergoes damage fracture, as shown in Fig.5b.

Adiabatic shear is an important phenomenon in titanium alloys under high strain rate loading conditions. At different temperatures, a flat shear band develops along the 45° direction (i. e., the direction of maximum shear stress) in Ti6321 titanium alloy. The width of its central shear band is shown in Fig.6. When the temperature is reduced from 298 K to 193 K, the average width of the shear band decreases from 6.76 μm to 3.56 μm, with a reduction of 47%. This variation in the shear band width is consistent with the prediction of Bai-Dodd theory[25,26]. Bai-Dodd theory predicts that the width of the shear band is:

$$\delta = 2\sqrt{\lambda T/\tau\gamma} \tag{3}$$

where $\lambda$ is the thermal conductivity, and $T$, $\gamma$, $\tau$ are the temperature, shear strain rate, and shear stress in the shear band, respectively. It shows that the width of the shear band decreases with decreasing temperature. This change is attributed to the combined effect of reduced thermal conductivity and specific heat capacity and increased rate of thermal softening. Firstly, it is mainly due to the shorter adiabatic heating process at low temperature. After adiabatic shear, the internal energy decreases sharply, resulting in a reduction in the width of the adiabatic shear band. Secondly, because the temperature decreases, the deformation resistance of the material increases, and the plastic deformation required for the shear zone is not generated inside the grain in time.

### 2.3 Deformation mechanism

The deformation of titanium alloys at low temperatures usually consists of a combination of two mechanisms, namely slip and twin. There are fewer slip systems for titanium alloys with hcp structure in the $\alpha$ phase and bcc structure in the $\beta$ phase. Therefore, it is difficult to initiate the slip system during plastic deformation. Gao et al[15] showed that industrial pure titanium TA2 can initiate the twin deformation mechanism when deformed at a high strain rate or low

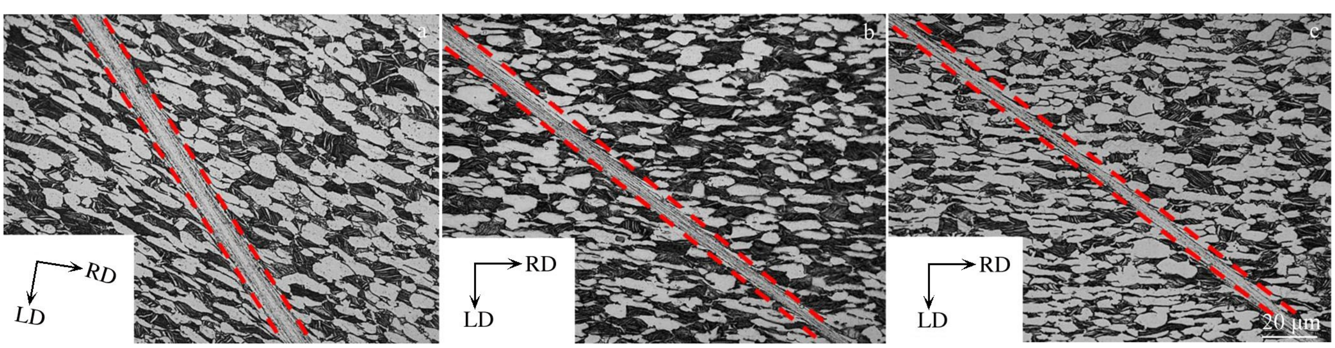


Fig.6 Adiabatic shear bands of Ti6321 alloy under different conditions: (a) 298 K, 2500 $s^{-1}$; (b) 253 K, 2500 $s^{-1}$; (c)193 K, 2500 $s^{-1}$

temperature, but there is a threshold value. The plastic deformation mechanism at high strain rate or low temperature is the combined deformation mechanism of twinning and slipping.

Fig. 7 shows the EBSD morphology after compression at different temperatures. Fig. 7a shows the structural morphology after compression at room temperature. The grain deformation at room temperature is small, the change in the grain boundaries is not obvious, and the number of observable twins is also small. Fig. 7b and 7c show the structure morphology after deformation at 253 and 193 K, respectively. The microstructure deformation is more serious as the temperature decreases, accompanied by grain fragmentation, and the number of observable twins increases. The increase in the number of twins indicates that twinning is an important mechanism for the deformation of Ti6321 titanium alloy at low temperature. In addition, twinning can change the orientation of the crystals, which can make some of the original unfavorable slip systems favorable to the occurrence of slip. Therefore, further slip and crystal deformation can be stimulated, and larger deformation can be produced by the joint action of slipping and twinning.

Fig. 7d, 7e and 7f show typical twins calibrated of Ti6321 alloy after deformation at different temperatures. By identification, the twins all appear in the $\alpha$ phase and are extended through the parent phase. The distribution of misorientation shows that there is a misorientation of approximately 86° between the twins calibrated in Fig. 7d and 7f and the parent phase, which corresponds to the commonest $\{10\bar{1}2\}$ $\langle\bar{1}011\rangle$ extension twins in titanium alloys. The misorientation of the calibrated twin in Fig. 7e with the parent phase is about 35°, which corresponds to the $\{11\bar{2}1\}\langle\bar{1}\bar{1}26\rangle$ extension twins commonly found in titanium alloys. It is consistent with the report of Chun[27]: $\{10\bar{1}2\}$ $\langle\bar{1}011\rangle$ are extension twins that occur over a wide range of temperatures, and $\{11\bar{2}1\}$ $\langle\bar{1}\bar{1}26\rangle$ is usually an extension twin that is activated at low temperatures or high strain rates.

Fig. 8a, 8b and 8c show TEM morphologies of Ti6321 alloy after dynamic compression at different temperatures. After deformation at room temperature, a large number of dislocations are observed in the structures, while there are fewer twins. Due to the rapid deformation process, dislocations do not have enough time to extend. A large number of dislocations gather between the $\beta$-sheet layers and form dislocation clusters. This result indicates that the deformation at room temperature is mainly based on dislocation slipping, and twinning deformation mainly plays a role in coordinating the deformation when slipping is difficult. A large number of twins are observed during low-temperature deformation at 253 and 193 K, as shown in Fig. 8b and 8c. This indicates that the deformation of Ti6321 titanium alloy at low temperatures is mainly dominated by twin deformation. Fig. 8d shows the HRTEM images of the nanosized twinning regions, in which the widths of the twinning bands are measured to be 4.66, 6.35, 4.76, 3.76, and 3.38 nm.

In general, the mechanism of compressive deformation of Ti6321 titanium alloy at room temperature (298 K) is mainly dislocation slipping. At 253 and 193 K, the compressive

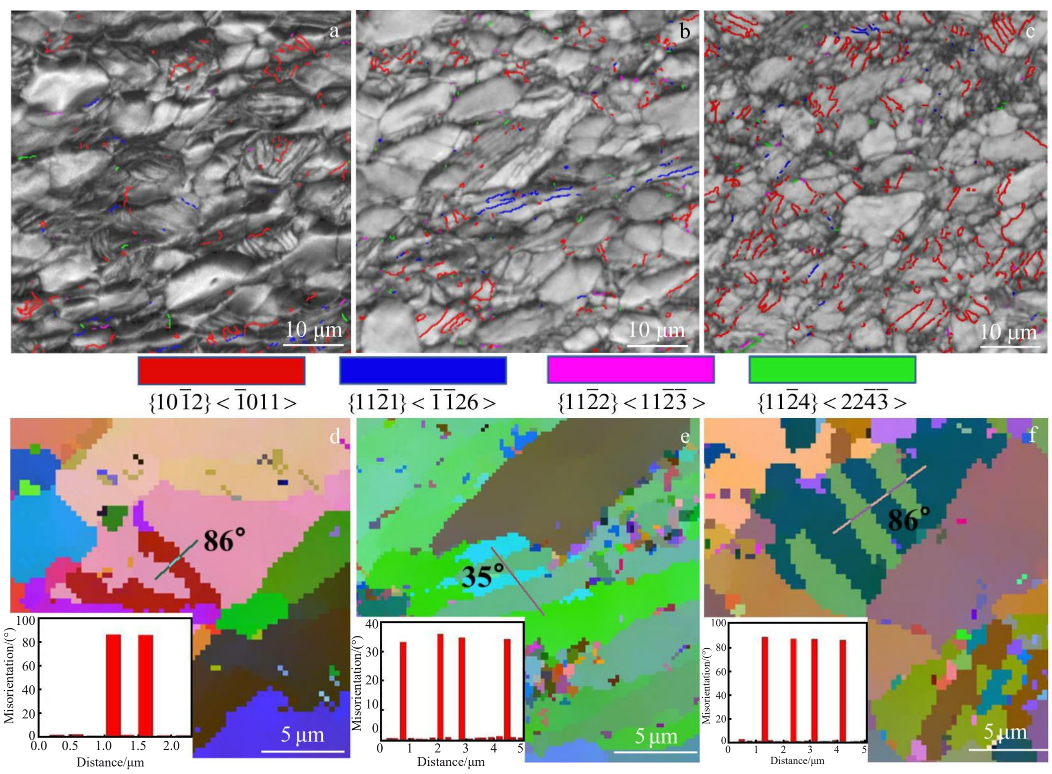


Fig.7 EBSD analysis of band contrast maps and twin identification (a~c) and Euler maps and misorientations of corresponding position (d~f) for Ti6321 titanium alloy at different temperatures: (a, d) 298 K, (b, e) 253 K and (c, f) 193 K

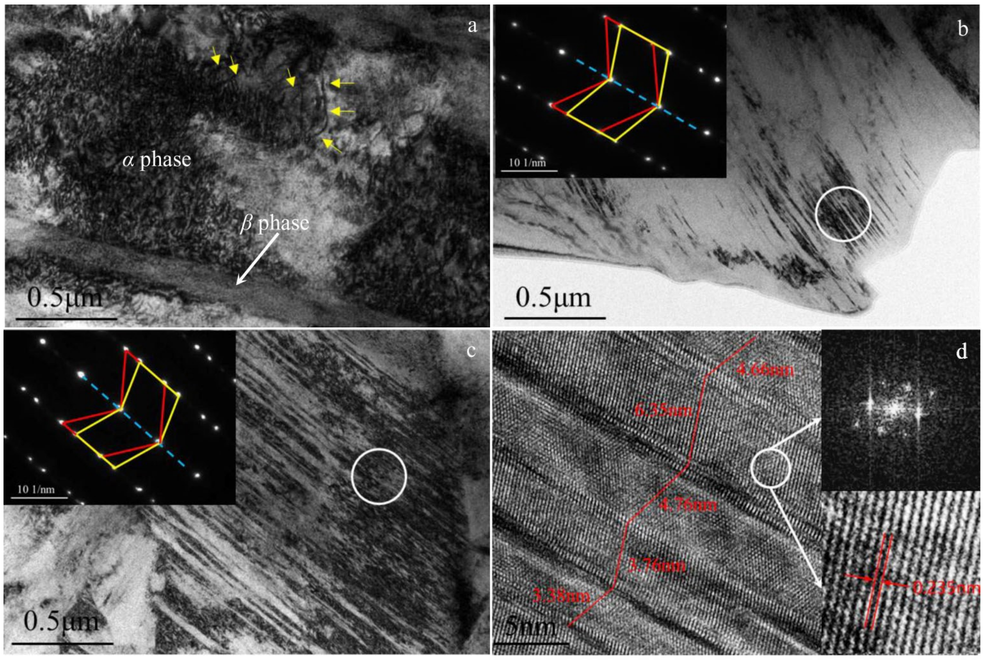


Fig.8 TEM images of Ti6321 alloy after dynamic compression at different temperatures: (a) dislocations at 298 K (shown by yellow arrow), (b) twinning with SAED pattern at 253 K, (c) twinning with SAED pattern at 193 K, and (d) HRTEM image of twin crystal regions

deformation mechanism of Ti6321 titanium alloy is a combination of twinning and slipping. The decrease in temperature makes the twinning active. Plastic deformation where dislocations are difficult to drive is complemented by twin deformation.

## 3 Conclusions

1) As the strain rate increases, the yield stress of Ti6321 titanium alloy rises, accompanied by an increase in flow stress and plastic strain, which causes the alloy to show a certain hardening effect under high strain rate loading condition. As the deformation temperature decreases, the strength increases, while the plasticity decreases.

2) The width of the shear band of Ti6321 alloy decreases with decreasing temperature. This difference is due to the combined effect of the decrease in thermal conductivity and heat capacity and the increase in thermal softening rate.

3) The main mechanism of compressive deformation of Ti6321 titanium alloy is dislocation slipping at room temperature (298 K), while it is a combination of twinning and slipping of dislocations at 253 and 193 K.

## References

1 Wang H, Sun Q Y, Xiao L *et al. Materials Science and Engineering A*[J], 2010, 527: 3493
2 Li G R, Qin T, Fei A G *et al. Journal of Alloys and Compounds*[J], 2019, 802: 50
3 Lin Junhui, Dan Zhenhua, Lu Jiafei *et al. Rare Metal Materials and Engineering*[J], 2020, 49(3): 1090 (in Chinese)
4 Xu Aijun, Wan Haifeng, Liang Chunzu *et al. Precision Forming Engineering*[J], 2020, 12(6): 145 (in Chinese)
5 Xiong Jinhui, Li Shikai, Gao Fuyang *et al. Materials Science and Engineering A*[J], 2015, 640: 419
6 Wang Q, Ren J Q, Wu Y K *et al. Journal of Alloys and Compounds*[J], 2019, 789: 249
7 Wang B F, Yao X R, Liu L Y *et al. Materials Science & Engineering A*[J], 2018, 736: 202
8 Song Dejun, Niu Long, Yang Shengli. *Rare Metal Materials and Engineering*[J], 2020, 49(3): 1100 (in Chinese)
9 Lu Zichuan, Sun Yachao, Yao Caogen *et al. Rare Metal Materials and Engineering*[J], 2022, 51(1): 217
10 Stéphane Di Iorio, Laurent Briottet, Edgar F Rauch *et al. Acta Materialia*[J], 2007, 55: 105
11 Huang Chaowen, Ge Peng, Zhao Yongqing *et al. Rare Metal Materials and Engineering*[J], 2016, 45(1): 254 (in Chinese)
12 Du Yu, Cai Xuezhang, Yang Guanjun. *Titanium Industry Progress*[J], 2005(6): 14 (in Chinese)
13 Zhang Jun, Wang Yang. *Materials Science and Engineering A*[J], 2014, 605: 59
14 Zhang Bin, Wang Yang. *Key Engineering Materials*[J], 2019, 794: 135
15 Gao Lingqing, Zhu Jinhua, Li Hui *et al. Rare Metal Materials and Engineering*[J], 2008, 38(6): 1051 (in Chinese)
16 Ning Zixuan, Wang Lin, Cheng Xingwang *et al. Acta Armamentarii*[J], 2021, 42(4): 862 (in Chinese)
17 Lu Zichuan, Zhang Xuhu, Ji Wei *et al. Materials Science & Engineering A*[J], 2021, 818: 141 380
18 Zang M C, Niu H Z, Yu J S *et al. Materials Science & Engineering A*[J], 2022, 840: 142 952

19 Zhou Dadi, Zeng Weidong, Xu Jianwei *et al. Materials Characterization*[J], 2019, 151: 103
20 Ning Zixuan, Wang Lin, Cheng Xingwang *et al. Ordnance Material Science and Engineering*[J], 2020, 43(6): 26 (in Chinese)
21 Nesar Ahmed Titu, Matt Baucum, Timothy No *et al. Procedia Manufacturing*[J], 2021, 53: 680
22 Wang Yuntian, Zeng Xiangguo, Chen Huayan *et al. Results in Physics*[J], 2021, 27: 104 498
23 Buzyurkin A E, Gladky I L, Kraus E I. *Aerospace Science and Technology*[J], 2015, 45: 121
24 He An, Xie Ganlin, Zhang Hailong *et al. Materials & Design*[J], 2013, 52: 677
25 Li Zezhou, Zhao Shiteng, Wang Bingfeng *et al. Acta Materialia*[J], 2019, 181: 408
26 Dodd B, Bai Y. *Materials Science and Technology*[J], 1989, 5(6): 557
27 Chun Y B, Battaini M, Davies C H J *et al. Metallurgical and Materials Transactions A*[J], 2010, 41(13): 3473

# Ti-6Al-3Nb-2Zr-1Mo钛合金在低温高应变速率下的变形行为

李严星[1]，王　琳[1,2,3]，安　瑞[1]，赵平洛[1]，闫志维[1]，程焕武[1,2]，程兴旺[1,2]

(1. 北京理工大学 材料学院，北京 100081)

(2. 北京理工大学 冲击环境材料技术国家级重点实验室，北京 100081)

(3. 北京理工大学 爆炸科学与技术国家重点实验室，北京 100081)

**摘　要：**在变形温度为193~298 K、应变速率为2000~3000 $s^{-1}$的范围内，对Ti6321钛合金进行动态压缩试验，研究温度和应变速率对材料力学性能和变形行为的影响。采用光学显微镜（OM）、透射电子显微镜（TEM）和电子背散射衍射（EBSD）表征和分析了合金的微观结构演变。结果表明，随着温度的降低和应变速率的增加，Ti6321钛合金的动态屈服强度和平均流动应力均增大，而断裂应变明显降低。采用Johnson-Cook本构方程预测了Ti6321钛合金在低温高应变速率下的力学行为，拟合结果与实验结果吻合较好。微观结构分析表明，随着变形温度的降低，{$11\bar{2}\bar{1}$}和{$10\bar{1}\bar{2}$}2种孪晶的含量明显增加，即变形机制逐渐由孪晶的辅助作用转变为孪晶占主导地位。

**关键词：**Ti-6Al-3Nb-2Zr-1Mo合金；低温；高应变速率；微观组织演化；变形机制

作者简介：李严星，男，1996年生，硕士生，北京理工大学材料学院，北京 100081，E-mail：1322174159@qq.com